Turkish Journal of Chemistry
http://journals.tubitak.gov.tr/chem/
Research Article

Turk J Chem
(2014) 38: 783 – 791

doi:10.3906/kim-1307-43

Study on transportation of phenol through a nanotubule membrane

Yue LIU, Li XIE, Xiaoxue FAN, Dingyan FAN, Shasheng HUANG*
Life and Environmental Science College, Shanghai Normal University, Shanghai, P.R. China

Received: 17.07.2013 • **Accepted:** 21.02.2014 • **Published Online:** 15.08.2014 • **Printed:** 12.09.2014

Abstract: Gold nanochannels were prepared by plating electrolessly gold within the pores of polycarbonate filter membranes (PCTMs). These PCTMs with cylindrical Au nanotubules of uniform radius and high density can be used as a convenient model system to investigate the mechanism of particle transport through nanotubules. The transport properties of phenol through a modified Au nanotubule membrane were studied. The permeate flux of phenol transport through the nanotubule membrane can be spatially and temporally manipulated by controlling the magnitude and direction of the current applied across the separation cell, and the electroosmotic flow (EOF) was investigated by measuring the flux of phenol across the PCTM. The current values and modification of nanotubules affected the EOF generated inside the nanotubules. The permeation flux of phenol through the nanotubule membrane can be easily changed by modifying the Au nanotubules with Cl^- or L-cysteine, and changing the direction of the applied current and the pH of the buffer solution used in mass transport experiments.

Key words: Au nanotubules, electroosmotic flow, transporting, phenol

1. Introduction

Molecular transport is of great practical significance in chemical analysis [1] and membrane separation technology. [2] Research on the transport and electrochemical properties of gold nanotubule membranes has received intensive attention. [3–9] It was found that Au nanotubes can be used as a convenient model system to investigate the mechanism of particle transport through a small space. Tubular structures are ideally suited for the transportation of chemical substances through nanotubule membranes because nanotubules are hollow and the inside and outside diameters of the tubes are controlled. Studies on the permeation of proteins, [10–12] DNA, [13,14] and some small organic molecules [15,16] through nanochannel membranes have been reported. The separation of the herbicides atrazine and paraquat based on modified Au nanotubule membranes has been investigated. [17]

In order to expand the possible application of nanotubule membranes in the membrane-based separation field, it is essential to maximize flux of molecules permeating through the membrane. Sun and Crooks studied the effect of diffusion and electrophoresis on the transportation of colloidal particles across single carbon-nanotube membranes. [18] Martin et al. reported that the flux of analyte transport through the membrane can be enhanced by electrophoresis or electroosmotic flow (EOF); they studied the EOF in template-prepared carbon nanotube membranes using phenol as a probe. [19]

Phenol, an important environmental pollutant, is a small molecule often used as a probe for electroosmotic measurements. [19] Here we report the transportation of phenol through a modified Au nanotubule membrane and

*Correspondence: sshuang@shnu.edu.cn

the EOF in nanotubule polycarbonate filtration membranes. The nanotubule membrane was used to separate 2 electrolyte solutions whereas an electrode in each solution was used to pass a constant ionic current through the nanotubules. The transportation of phenol through the membrane can be represented by the permeation flux of phenol. By controlling the magnitude and direction of the applied current, the mass transport through these nanotubule membrane can be spatially and temporally manipulated due to the EOF generated in nanotubules. Further investigation was performed for Au nanotubule membranes modified with L-cysteine[15,20] or Cl^-.[20] As a result, the permeation flux should be easily changed by modifying the Au nanotubules and changing the direction of the applied current and the pH of the buffer solution used in mass transport experiments. Studies of mass transportation of phenol through nanotubules may help us to understand the pore surface characters and provide an alternative method for chemical and biological separations.

2. Results and discussion

2.1. Characterization of Au nanotubule membrane

When an electroless plating method is used to deposit Au onto the wall of pores of polycarbonate nanoporous filtration membranes, the diameter of the nanochannels may be controlled by the plating time. Figure 1 shows the FE-SEM of PCTM with pore diameter of 100 nm (Figure 1a), the Au nanotubule membrane with 7 h deposition (Figure 1b), and the Au nanotubule membrane modified with L-Cys (Figure 1c). From Figure 1, it can be seen that the diameter of pores after depositing for 7 h was obviously less than that of PCTM. After modifying with L-Cys, the surface of the PCTM was covered with some organic molecular clouds, indicating that the modification was successful. In order to investigate the morphology of the nanochannels, after plating for 7 h, the Au nanochannel membrane was dissolved in dichloromethane. TEM of dichloromethane solution showed that Au nanotubules in good shape can be obtained in this way (Figure 1d).

2.2. Transportation of phenol through Au nanotubule membrane at different applied currents

Figure 2 shows a plot of phenol flux transported through the Au nanotubule membrane (curve A) at various applied transmembrane currents in a 0.01 M phosphate buffer solution (pH 7.2). Five linear segments were obtained (curve A in Figure 2), and the slope of each segment was the flux of phenol (N_J) at that applied current (Table 1). The first linear segment in curve A (0 to 40 min, segment a) was obtained with no applied current, and the flux in this case was simply the diffusive flux of phenol, N_{diff}, from the feed half-cell across the membrane and into the permeate half-cell. The second linear segment (40 to 80 min, segment b) was obtained with an applied current, J_{app} = 0.25 mA. The flux of phenol transport through the membrane increased in comparison with N_{diff}. When a negative current, J_{app} = –0.25 mA, was applied, the net flux of phenol (the segment c (80 to 120 min)) was lower than the diffusive flux obtained at no applied current. The final 2 linear segments of curve A were obtained at higher positive and negative applied currents, respectively. From the final 2 linear segments of curve A, the flux of phenol at 0.5 mA applied current (segment d) was further enhanced, and a diminution of flux at –0.5 mA applied current (segment e) can be observed.

When an external electrical field is applied in the direction tangential to the surface with an electrical double layer (EDL), the fluid will be dragged by the EDL and generate an EOF. From Figure 2, it can be seen that the flux of phenol was higher than diffusion flux when a positive current was applied, indicating that the direction of EOF was the same as the diffusion flux (EOF from feed solution to permeate solution). In this case, the surface of the fluid was positively charged and the inner wall of the Au nanotubules was negatively charged.

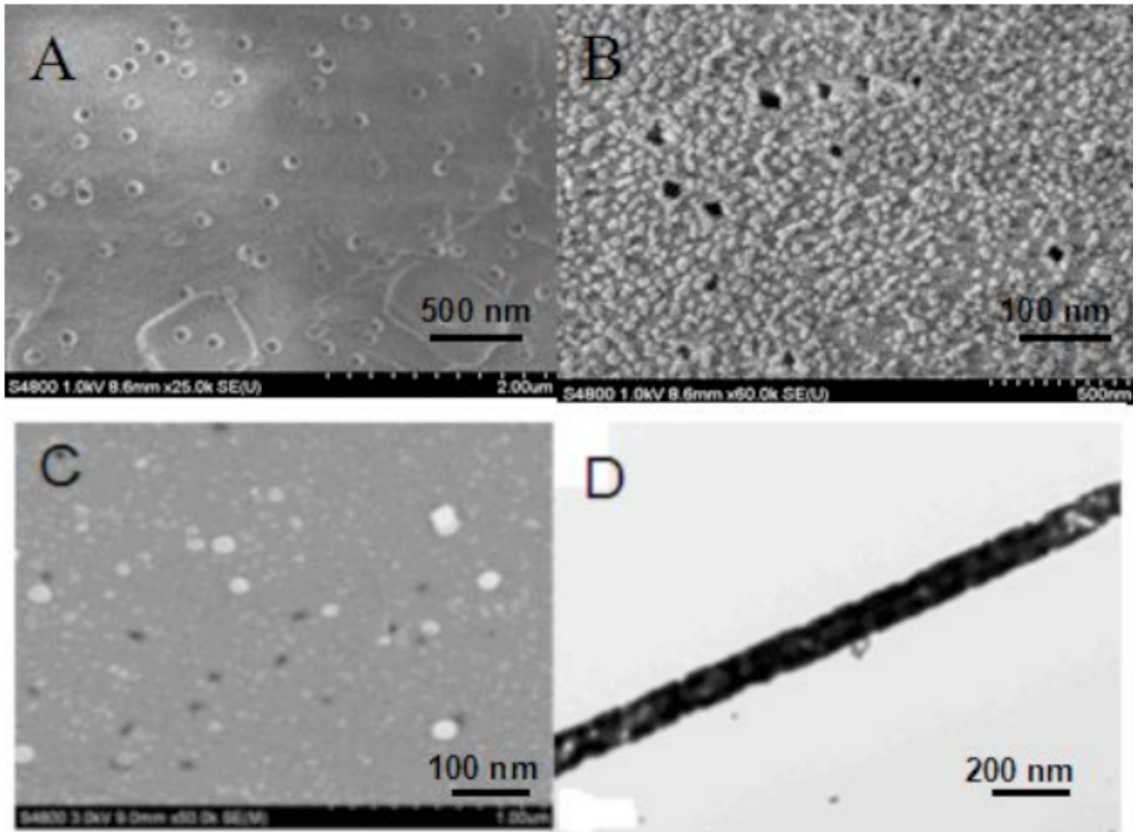

Figure 1. FE-SEM images of PCTE membrane (A), Au membrane with 7 h deposition (B), and the Au nanotubule membrane was modified with Cys (C). TEM of the Au-nano pipes (D, the Au-nanochannel membrane was solved in dichloromethane after plating for 7 h).

Table 1. Effect of applied current on the flux, enhancement factor, and electroosmotic velocity in the Au nanotubule membrane in pH 7.2 phosphate buffer solution.

I, mA	Flux, nmol/(min cm^2)*	E	Pe	v_{eo}, μm/s
–0.50	11.0 ± 0.21	0.224	–2.497	–402.9
–0.25	21.0 ± 0.44	0.437	–1.477	–238.3
0	49.0 ± 0.78	1.000	0	0
0.25	98 ± 1.5	2.000	1.594	257.1
0.50	130 ± 1.5	2.656	2.420	390.4

*n = 3. The data were obtained in 0.01 M pH 7.2 phosphate buffer.

Figure 3 shows that the zeta potentials of Au nanopipes and Au nanopipes modified with L-Cys were –16.5 mV and –30.4 mV, respectively, indicating that the surface of the nanotubules was indeed negatively charged.

2.3. Calculation of the electroosmotic velocity

In the presence of the applied transmembrane current, the mass across a membrane is governed by the Nernst–Planck equation.[18,21] For a one-dimensional system, the mass transfer (N_J) along the x-axis can be written as

$$N_J = -D\frac{\partial C(x)}{\partial x} - \frac{zF}{RT}DC\frac{\partial \phi(x)}{\partial x} + Cv_{eo}(x), \quad (1)$$

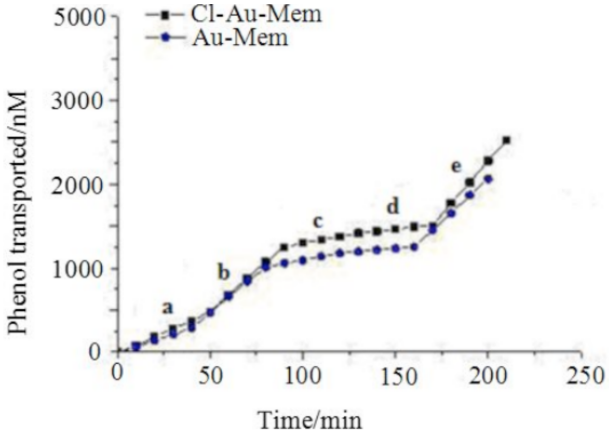

Figure 2. Phenol flux as a function of time at applied transmembrane current across Au nanotubule membrane. Curve A, Au-mem; curve B, Cl-Au-mem. Applied current: a, 0 mA; b, 0.25 mA; c, –0.25 mA; d, 0.5 mA; e, –0.5 mA.

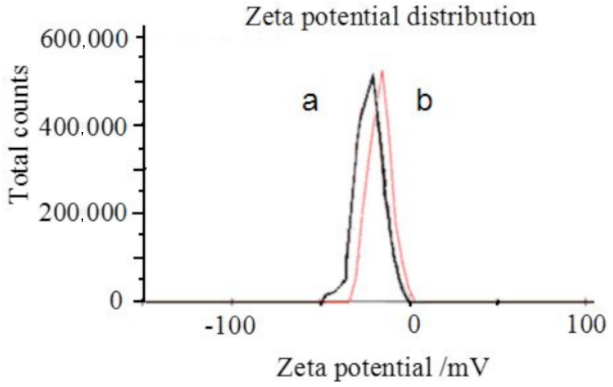

Figure 3. Zeta potential distribution of Au nanotubules modified with L-cysteine (a) and Au nanopipes (b).

where D, C, and z are the diffusion coefficient, concentration, and charge of the permeate molecule, respectively. ∂C(x)/∂x is the concentration gradient in the x direction across the membrane, $\partial\varphi$(x)/∂x is the potential gradient in the electrolyte within the nanotubules, and v_{eo} is the electroosmotic velocity. The 3 terms in Eq. (1) describe the diffusive, migration, and EOF convective transport processes, respectively. Because phenol is a neutral molecule at the pH used here (pH 7.2), Eq. (1) simplifies to

$$N_J = -D\frac{\partial C(x)}{\partial x} + Cv_{eo}(x) \tag{2}$$

when $J_{app} = 0$, only the first term in Eq. (2) is operative and the flux is the diffusive flux, N_{diff}.

$$N_{diff} = -D\frac{\partial C(x)}{\partial x} \tag{3}$$

The flux data obtained in the experiments can be used to calculate a parameter called the enhancement factor, E, which can then be used to calculate the electroosmotic velocity. E is given by

$$E = N_J/N_{diff} \tag{4}$$

i.e. the ratio of the flux in the presence of an applied current to the flux at $J_{app} = 0$.

According to Srinivasan and Higuchi, [22] the Péclet number (Pe) can be calculated from E via

$$E = \frac{Pe}{1 - e^{-Pe}}. \tag{5}$$

Pe can then be used to calculate v_{eo} using

$$v_{eo} = Pe(D/l), \tag{6}$$

where D is the diffusion coefficient and l is the thickness of the membrane. According to Martin, [19] because the inside diameter of the Au nanotubules (~60 nm) is much larger than the size of phenol (~0.24 nm), hindered diffusion does not occur in these tubes, and the bulk solution diffusion coefficient can be used in Eq. (6). v_{eo}, calculated from Pe, D, and l, is shown in the last column in Table 1. As expected, current densities of the same magnitude but opposite sign give v_{eo} values of approximately the same magnitude but opposite sign.

2.4. Effect of applied current on electroosmotic velocity

The standard equation describing the velocity (v_{eo}) in an electroosmotic driven open capillary system is as follows:[23]

$$v_{eo} = \frac{\varepsilon_0 \varepsilon_r \zeta}{\eta} \frac{U}{l}, \tag{7}$$

where η is the viscosity of the fluid, ε_0 is the electrical permittivity of the vacuum, ε_r is the relative permittivity of the medium (or dielectric constant), ζ is the zeta potential at the capillary wall, and U is the voltage applied across the capillary with a length of l.

Introducing the resistivity of the electrolyte (ρ) within the nanopores for the applied voltage into Eq. (1) gives

$$v_{eo} = \frac{\varepsilon_0 \varepsilon_r \zeta}{\eta} \frac{\rho}{l} I \tag{8}$$

Eq. (2) shows that v_{eo} is linearly related to the applied current. Eqs. (5) and (6) were used to calculate v_{eo} from the flux data in Table 1.

It should be noted that Eqs. (7) and (8) can be used based on the assumption that the thickness of the double layer at the pore wall is much less than the pore radius. Because the double layer at this electrolyte concentration is less than 3 nm in thickness,[24] this is clearly a valid assumption.

2.5. Effect of modification of nanotubules on EOF

2.5.1. EOF in Cl^--Au nanotubule membrane

Cl^- can be strongly adsorbed on Au.[20] Au nanotubules can be modified by Cl^- ion due to the strong adsorption of Cl^- on the wall of pores.[25,26] For the Cl^--Au-Mem, the transportation of phenol through this nanotubule membrane was similar to that for the Au-Mem.

The curve B in Figure 2 depicts the plot of phenol flux transported through the Cl^--Au-Mem at various applied transmembrane currents in 0.01 M PBS (pH 7.2) at different applied currents. The first linear segment (0 to 50 min, segment a) in curve B was obtained with no applied current, and the flux was the diffusive flux of phenol, N_{diff}. The second linear segment (50 to 90 min, segment b) was obtained with an applied current, $J_{app} = 0.25$ mA. It can be seen that the flux of phenol across the Cl^--Au-Mem increased, indicating that EOF was in the same direction as the diffusive flux. When a negative current, $J_{app} = –0.25$ mA, was used (segment c, 90 to 130 min), the net flux was lower than the diffusive flux, indicating that EOF was in the opposite direction to diffusive transportation. The final 2 linear segments were obtained at higher positive and negative applied currents, and further enhancement and diminution in the flux are observed, respectively.

However, from Figure 2, it can be seen that the difference between the fluxes of phenol at the positive polarity and N_{diff} was obviously larger than that between the fluxes of phenol at the negative polarity and N_{diff}. Perhaps, besides the diffusive flux and EOF, the fluxes of phenol through the nanotubules were affected by electromigration flux due to the partial protonation of phenol in the pores in this case.

2.5.2. Effect of surface properties of the nanotube membranes on v_{eo}

From Eq. (1), it is clear that the diffusion, migration, and convection processes are highly coupled and depend largely on the charge and diffusivity of the permeation molecule as well as the physical characteristics of the

medium containing the permeation molecule being transported. In this section, a discussion will be given with respect to the membranes modified with L-cysteine.

L-cysteine, with an isoelectric point of 5.2, is often used in nanotubules as a modifier due to its –SH group. It can be chemisorbed onto Au nanotubules via this –SH group.[5] The electric feature of the nanotubules chemisorbed by L-cysteine depends on the solution pH. Under the condition of low pH, the inner wall of nanotubules of the Cys-Au-Mem have excess positive charge due to the protonation of the amino group, and the feature of EOF under this condition is opposite to those in the Cl^--Au-Mem when currents are used on the separation cell. At the isoelectric point of L-cysteine, there is no net charge on the surface of nanotubules, i.e. v_{eo} equals zero. At high pH, due to the deprotonation of carboxyl, the membrane is negatively charged. In this case, the feature of EOF is the same as that in the Cl^--Au-Mem when a current is applied. Figure 4 shows the alteration of Cys adsorbed on the wall of nanotubules with change in medium pH.

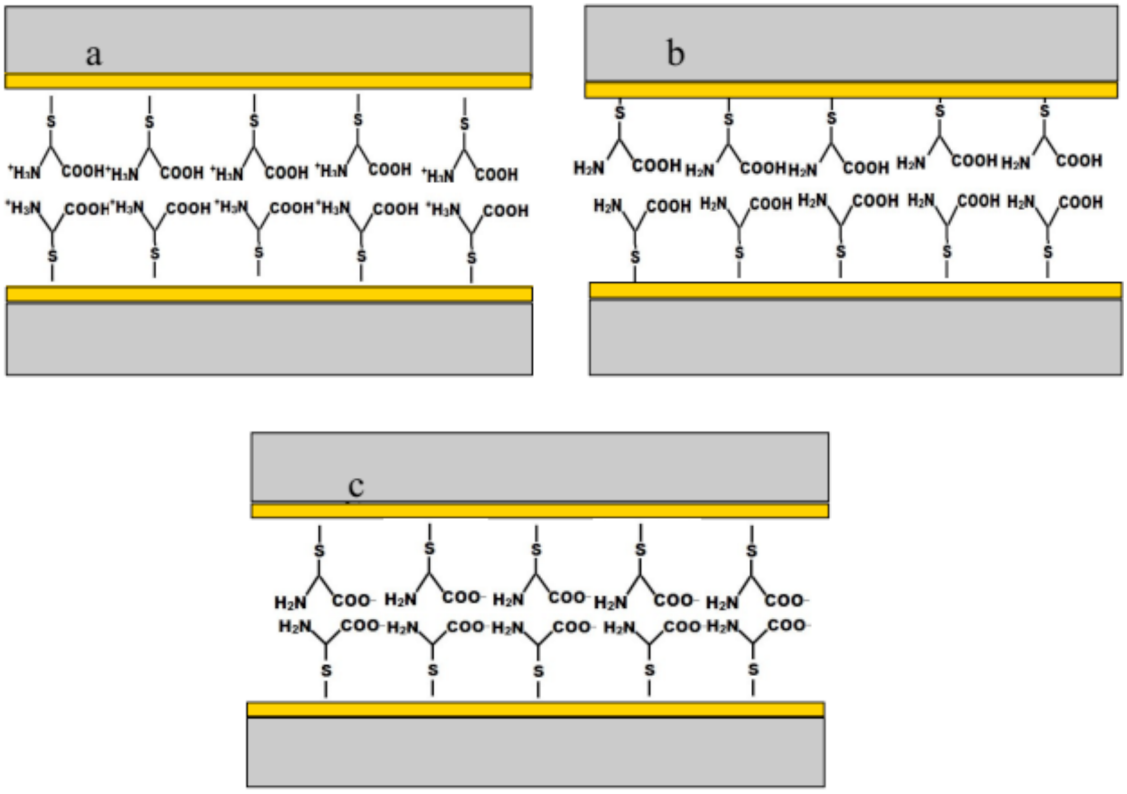

Figure 4. Schematic representation showing the 3 states of protonation of the chemisorbed cysteine. a: low pH, protonated amino group; b: isoelectric point, protonated amino and deprotonated carboxyl; c: high pH, deprotonated carboxyl.

Table 2 shows the flux of phenol transported across the Cys-Au-Mem at various applied currents in 0.01 M phosphate buffer solution, and pH of the buffer solution was adjusted to values of 2 $\sim$ 7.2. From Table 2, it can be seen that the flux of phenol through the Cys-Au-Mem at pH 5 and pH 7 (the inner wall of nanotubules was negatively charged in this case) increased with the increase in applied current when a positive current was used, and the flux decreased with the increase in applied current when a negative current was applied. Opposite results were obtained at low pH (pH 2, pH 3) due to the positively charged inner walls.

From Table 2, it can be seen that the flux of phenol across the membrane increased with increasing

positive current at pH 4.0; this might be attributed to the negative sites introduced by deprotonation of the carboxyl group. However, an unexpected feature can be seen from the data in Table 2 at pH 4.0. The change trend of the flux of phenol obtained at pH 4.0 was different from those obtained in lower pH media or in higher pH media when a negative current was applied. The data of phenol flux in Table 2 were not an experimental error because we did this experiment many times and this trend can be repeated. The reason for these experimental results may be as follows. Firstly, according to Belkova et al.,[27] the pH values in narrow pores can significantly differ from those in the bulk solution. Secondly, L-cysteine is a weak electrolyte. Apart from dependency of the dissociation constant of weak electrolyte in constrained volumes with charged walls, the pH in the L-cysteine–modified narrow pores can be influenced by the L-cysteine itself because the surface density of L-cysteine on the walls is high enough. Thirdly, the fact that phenol in the pores may be partially protonated leads to the experimental results that the more acidic was in the medium, the more clear was the "asymmetry" of phenolic "+" and "–" fluxes.

Table 2. Phenol flux transported across Cys-Au-Mem at various pH values in 0.01 M phosphate buffer solution*.

I, mA	pH 2.0	pH 3.0	pH 4.0	pH 5.0	pH 7.2
–0.50	54 ± 3.6	43 ± 1.8	37 ± 1.6	8.0 ± 0.9	13 ± 1.1
–0.25	50 ± 2.4	38 ± 1.6	13 ± 1.4	16 ± 1.1	22 ± 1.9
0	49 ± 2.5	37 ± 2.5	36 ± 1.5	41 ± 1.4	40 ± 2.2
0.25	31 ± 1.6	34 ± 1.9	52 ± 2.9	62 ± 1.5	74 ± 3.7
0.50	28 ± 1.2	34 ± 3.7	89 ± 5.8	98 ± 4.9	96 ± 4.8

*n = 3

3. Experimental

3.1. Materials

Polycarbonate nanoporous filtration membranes with pore diameters of 100 nm, thickness of 6 μm, and pore densities of 6×10^8 pores/cm^2 (PCTM, Whatman Company, UK) were used to prepare Au nanochannels. Phenol was provided by Shanghai Chemical Reagent Company. Milli Q 18.2 MΩ water was used throughout the experiment. Phosphate buffer solutions (PBS) with various pH values ($2 \sim 7.2$) were prepared with 0.01 M Na_2HPO_4 and 0.01 M NaH_2PO_4. All the chemicals used in the experiments were of analytical grade.

A field emission scanning electron microscope (FE-SEM, JSM-6700F, Japan) was used to characterize the nanotubules. The figures of transmission electron microscopy (TEM) were obtained with a JEM-2010 (JEOL, Japan). An ultraviolet spectrograph UV-2102C (Shanghai, PR China) was used to record UV absorption. Zeta potential was measured by a Zeta potential analyzer (ZEN 3600, Malvern).

3.2. Procedure

3.2.1. Preparation of the Au nanotubules

Au nanotubules were prepared according to the modified method proposed by Menon and Martin.[28] The polycarbonate nanoporous filtration membrane was immersed in methanol for 5 min and then immersed in a methanol solution of 0.025 M $SnCl_2$ and 0.07 M tri?uoroacetic acid for 45 min. The membrane was then placed in methanol twice, each for 2.5 min, and then immersed in an aqueous ammoniacal $AgNO_3$ solution (0.029 M) for 5 min, followed by soaking in methanol for 5 min. After treatment in $AgNO_3$, the membrane was placed in a gold-plating bath containing 7.9×10^{-4} M $NaAu(SO_3)_2$, 0.127 M Na_2SO_3, 0.625 M formaldehyde, and

0.025 M $NaHCO_3$. The temperature of this bath was maintained at 5 °C. The plating solution was adjusted to pH 10.87 by dropwise addition of 0.5 M H_2SO_4 with constant stirring. The Au nanotubule membrane was immersed in 25% (v/v) nitric acid to remove impurities adsorbed on the surface of the membrane, followed by rinsing with water twice.

3.2.2. Modification of the Au nanotubules

The surface modification of the inner wall of tubes of Au nanotubules was carried out by immersing the nanotubule membrane in a solution containing 0.1 M KCl or 1.0 mM L-cysteine for 24 h at room temperature in a nitrogen atmosphere, and then rinsing with PBS buffer solution to remove the unnecessary KCl or L-cystine. In this paper, Au-Mem, Cl^--Au-Mem, and Cys-Au-Mem were used to denote the polycarbonate nanoporous filtration membrane covered with gold, the Au-nanotubule membrane modified with Cl^-, and the Au-nanotubule membrane modified with L-Cys, respectively. In this work, a nanoporous membrane with diameter of 100 nm was used and the diameter of gold nanochannels was about 60 nm after electrolessly depositing for 7 h.

3.2.3. Transport experiments

The apparatus used for the transport experiments nanochannels was the same as that described before.[15] The membrane was mounted between 2 halves of a U-tube permeate cell; 10 mL of phosphate buffer solutions with different pH containing 5.0 mM phenol to be tested was put into the feed cell while buffer solution of the same volume as the to-be-tested solution was put into the permeate cell to keep the same height of liquid surface in both cells (the effective permeation area of membrane was 0.196 cm^2). During the transport experiment, a constant current, J_{app}, was driven through the membrane using 2 platinum electrodes with a DJS-292 B galvanostat. A 3.0 V potential value was applied during the transport experiments. The transport flux was accomplished by determining the absorption of solution in the permeation cell at 270 nm. As described in Martin's report,[19] the sign convention employed in this report was as follows: when a positive applied current, J_{app}, was used, the anode of the galvanic circuit was in the feed half-cell and the cathode was in the permeate half-cell. Thus, the cations migrated from the feed half-cell to permeate and anions from the permeate half-cell to feed. Conversely, when a negative applied current, J_{app}, was used, the cathode was in the feed half-cell and the anode was in the permeate half-cell. Each experiment was repeated 3 times except when stated otherwise.

4. Conclusions

It is shown that EOF can be driven across Au nanotube membranes and the rate and direction of flow should be easily controlled by means of suitable modification of Au nanotubules, the magnitude and sign of the applied current, and the pH of the buffer solution used in mass transport experiments. L-cysteine can be chemisorbed onto the Au nanotubules via its –SH and this provides another route for adjusting the rate and direction of EOF. The controllability and diversity of the nanotubules' inner surface and electroosmotic property enable the possible application of nanotubule membranes in the field of chemical/biological separation.

Acknowledgments

This work was supported by the Project of the National Science Foundation of People's Republic of China (21275100), Shanghai Leading Academic Discipline Project (S30406), and Key Laboratory of Resource Chemistry of Ministry of Education.

References

1. Jorgenson, J. W.; Lukacs, K. D. *Anal. Chem.* **1981**, *53*, 1298–1302.
2. Sourirajan, S.; Matsuura, T. *Reverse Osmosis and Ultrafiltration*; American Chemical Society: Washington DC, USA, 1985.
3. Hulteen, J. C.; Jirage, K. B.; Martin, C. R. *J. Am. Chem. Soc.* **1998**, *120*, 6603–6604.
4. Jirage, K. B.; Hulteen, J. C.; Martin, C. R. *Anal. Chem.* **1999**, *71*, 4913–4918.
5. Lee, S. B.; Martin, C. R. *Anal. Chem.* **2001**, *73*, 768–775.
6. Che, G.; Miller, S. A.; Fisher, E. R.; Martin, C. R. *Anal. Chem.* **1999**, *71*, 3187–3191.
7. Martin, C. R. *Science* **1994**, *266*, 1961–1966.
8. Mubarak, A.; Basit, Y.; Reinhard, N.; Wolfgang, E.; Wolfgang, K.; Omar, A. *J. Am. Chem. Soc.* **2008**, *130*, 16351–16357.
9. Dujardin, E.; Ebbeson, T. W.; Hiura, H.; Tanigaki, K. *Science* **1994**, *265*, 1850–1852.
10. Yu, S. F.; Lee, S. B.; Martin, C. R. *Anal. Chem.* **2003**, *75*, 1239–1244.
11. Huang, S. S.; Sheng, C.; Yin, Z. F.; Shen, J.; Li, R. N.; Peng, B. *J. Memb. Science* **2007**, *305*, 257–262.
12. Huang, S. S.; Yin, Z. F.; Yang, X. H.; Wang, K. M.; Tan, W. H.; He, X. X.; Zhong, T. *Chinese J. Anal. Chem.* **2006**, *34*, 1515–1518.
13. Huang, S. S.; Yin, Y. F.; Wang, K. M.; He, X. X.; Zhong T. S. *Chem. J. Chinese U.* 2004, *25*, 2238–2241.
14. Mitchell, D. T.; Lee, S. B.; Trofin, L.; Li, N.; Nevanen, T. K.; Söderlund, H.; Martin, C. R. *J. Am. Chem. Soc.* **2002**, *124*, 11864–11865.
15. Kohli, P.; Harrell, C. C.; Cao, Z. H.; Gasparac, R.; Tan, W.; Martin, C. R. *Science* **2004**, *305*, 984–986.
16. Huang, S. S.; Yin, Y. F. *Anal. Sci.* **2006**, *22*, 1005–1009.
17. Jirage, K. B.; Hulteen, J. C.; Martin, C. R. *Science* **1997**, *78*, 655–658.
18. Yue, Z. L.; Zhao, G. Q.; Huang, S. S.; Fan, X. X.; Shi, W. L.; Zhang, Z. H. *J. Memb. Sci.* **2010**, *356*, 117–122.
19. Sun, L.; Crooks, R. M. *J. Electrochem. Soc.* **2000**, *122*, 12340–12345.
20. Miller, S. A.; Young, V. Y.; Martin, C. R. *J. Am. Chem. Soc.* **2001**, *123*, 12335–12342.
21. Biggs, S.; Mulvaney, P.; Zukoski, C. F.; Grieser, F. *J. Am. Chem. Soc.* **1994**, *116*, 9150–9157.
22. Bath, B. D.; White, H. S. *Anal. Chem.* **2000**, *72*, 433–442.
23. Srinivasan, V.; Higuchi, W. I. *Int. J. Pharm.* **1990**, *60*, 133–138.
24. Knox, J. H.; Grant, I. H. *Chromatographic* **1987**, *24*, 135–143.
25. Probstein, R. F. *Physicochemical Hydrodynamics: An Introduction*; Buttersworth Publishers: Stoneham, MA, USA, 1989.
26. Nishizawa, M.; Menon, V. P.; Martin, C. R. *Science* **1995**, *268*, 700–702.
27. Wang, Y. R.; Hu, P.; Liang, Q. L.; Luo, G. A.; Wang, W. M. *Chinese J. Anal. Chem.* **2007**, *35*, 583–585.
28. Belkova, A. A.; Sergeeva, A. I.; Apel, P. Y.; Beklemishev, M. K. *J. Memb. Sci.* **2009**, *330*, 145–155.
29. Menon, V. P.; Martin, C. R. *Anal. Chem.* **1995**, *67*, 1920–1928.